IEEE Access
Multidisciplinary | Rapid Review | Open Access Journal

Received 6 February 2023, accepted 23 February 2023, date of publication 27 February 2023, date of current version 2 March 2023.

Digital Object Identifier 10.1109/ACCESS.2023.3249963

RESEARCH ARTICLE

A Broadband Full-Corporate-Fed Slot Array Antenna Based on the Single-Layer Substrate Integrated Waveguide

BAOQUAN DUAN[1,2], (Graduate Student Member, IEEE), SHIJIU ZHENG[2], MIAO ZHANG[2], (Senior Member, IEEE), JIRO HIROKAWA[1,2], (Fellow, IEEE), AND QING HUO LIU[2,3], (Fellow, IEEE)

[1]Department of Electrical and Electronic Engineering, Tokyo Institute of Technology, Tokyo 152-8552, Japan
[2]Institute of Electromagnetics and Acoustics, Xiamen University, Xiamen 361005, China
[3]School of Electronic Science and Technology, Eastern Institute for Advanced Study, Ningbo 315200, China

Corresponding author: Miao Zhang (miao@xmu.edu.cn)

This work was supported in part by the National Natural Science Foundation of China under Grant 61971364; and in part by the Fundamental Research Funds for the Central Universities, Xiamen University, under Grant 20720170052.

ABSTRACT A single-layer corporate-fed substrate integrated waveguide slot array antenna is newly proposed and verified. It is characterized by low profile, easy fabrication, low cost, low sidelobes, wideband operation, and high efficiency. A V-band 16 × 16-element array with uniform excitation is designed for demonstration. The radiating elements and feeding waveguides are arranged within a single-layer substrate, whose dielectric constant and loss tangent are appropriately selected. By adopting the full-corporate feed, the 16 × 16 radiating slots are excited by the 16 × 16 output ports of the feeding circuit, which is composed of cascaded H-plane T-junctions. For further bandwidth improvement, a metal grid plate is introduced on the top of the radiating slots. The test antenna is fabricated by the conventional PCB process. The measured bandwidth for $|S_{11}| < -10$ dB is 16.2%, fully covering the 57–67 GHz frequency range. Meanwhile, the measured antenna gain higher than 30 dBi associated with the antenna efficiency higher than 45% is achieved over the 58−65 GHz frequency range.

INDEX TERMS Slot array antenna, substrate integrated waveguide, single-layer structure, full corporate feed, broadband design.

I. INTRODUCTION

In recent years, the high-gain and high-efficiency antennas have become crucial devices for various wireless communication and radar systems. Due to the strong oxygen absorption and the high propagation path loss in the millimeter-wave (mmW) band, it has been reported in [1] that the 60-GHz-band array antenna with a gain higher than 30 dBi is indispensable when the communication distance is longer than 100 m. Meanwhile, a broadband antenna is in high demand in the point-to-point high-speed fixed wireless access system [2], adopting a wide frequency band. Lens antennas [3] and reflector antennas [4] with large apertures are the typical candidates. They enjoy the features of high gain, high efficiency, and wideband operation, but simultaneously suffer from weight and volume issues.

The planar array antennas would be the effective solutions. In particular, the hollow waveguide slot array antenna and the gap waveguide slot antenna have advantages over the microstrip line-fed array antenna [5] in terms of both dielectric loss and radiating loss. On the other hand, the long-line effect [6] is the main factor determining the bandwidth of array antennas. The feeding circuits of the waveguide slot arrays have evolved from the center-fed single-layer structure [7] into the partially corporate-fed [8] and the corporate-fed [9], [10] double-layer structures. The bandwidth has been improved from a few percent to around 20% step by step.

The associate editor coordinating the review of this manuscript and approving it for publication was Tutku Karacolak.

Therefore, a corporate-feed structure is preferred in a high-gain antenna design.

A high-gain and high-efficiency corporate-fed slot array based on conventional hollow waveguide technology in the 60-GHz band has been reported in [9]. A process called ''diffusing bonding of laminated thin plates'' has been introduced in the successful realization of hollow waveguide slot array antennas, especially in the mmW-band. Another high-gain and high-efficiency planar antenna is based on the ridge gap waveguide technique [11], [12], which eliminates the high demand for perfect electric contact between metal components. However, the traditional milling process for prototyping is still costly and time-consuming.

As a closed and planar waveguiding structure with merits of low loss, low fabrication cost, and low profile, the dielectric-filled post-wall waveguide, as well as substrate integrated waveguide (SIW), is born as a promising candidate for mmW applications. So far, various SIW corporate-fed array antenna has been studied by many researchers. For example, a SIW cavity-backed array antenna [13], cavity-backed patch antenna arrays with full-corporate SIW feeding networks [14], [15], and a SIW-fed cavity array antenna based on LTCC [16] have been developed. All of those corporate-fed array antennas, based on the hollow waveguide [9], ridge gap waveguide [11], and SIW [13], [14], [15], [16], adopt the double-layer cavity-backed structures. Hence, the radiating unit becomes a 2×2-element or 1×2-element subarray rather than a single slot. Those slots within one subarray share the same cavity and are uniformly excited. However, due to their symmetry, there exist grating lobes when adopting amplitude tapers [17] to suppress sidelobes. Meanwhile, it is also inevitable to increase the manufacturing cost and the design complexity when dealing with those double-layer corporate-fed SIW antennas.

On the other hand, two types of single-layer corporate-fed slot arrays, based on the hollow rectangular coaxial line [16] and ridge gap waveguide [19], [20], have been proposed in the V-band. By shrinking the cross-section of transmission lines, the radiating unit becomes a 1×1-element subarray. However, in a hollow rectangular coaxial line, additional structures were introduced to support the inner conductors. They increased the fabrication complexity and degraded the matching bandwidth. The measured bandwidth for $|S_{11}|<-12.5$ dB was about 8.3% only, and the measured peak antenna efficiency maintained as high as 76.3%. In [19], relatively good antenna performance has been achieved in a single-layer corporate-feed ridge gap waveguide slot array. However, the misalignment degraded the matching performance, and the fabrication process is still costly and time-consuming. In [21], a full-corporate-fed patch array based on the SIW structure was realized. The wideband characteristic is achieved by a multiple-layered array, and its scale was quite limited. Therefore, considering both fabrication cost and processing time, there is still a high demand for the large-scale single-layer full-corporate-fed SIW slot array antenna.

According to the reasons illustrated above, this paper originally introduces a single-layer full-corporate-fed slot array antenna based on the SIW technique. It is characterized by low profile, easy fabrication, low cost, low sidelobes, wideband operation, and high efficiency. Previously, the Rogers substrate RT/duroid 6002 has been verified as a promising candidate [22], where a subarray fed by the dielectric-filled waveguide was demonstrated. The waveguides' dimensions are appropriately shrunk to arrange both radiating elements and feeding waveguides within a single-layer substrate. Thus, the radiating unit becomes the single radiating slot, and both its exciting amplitude and phase can be independently controlled. Generally, strong mutual coupling among slots may drastically degrade the bandwidth of the radiating units. According to our investigation, a metal grid plate, which possesses periodically arranged open air-cavities, is newly introduced on top of the substrate to improve bandwidth performance significantly.

A 16×16-element single-layer full-corporate-fed SIW slot array with uniform excitation is designed in the V-band for demonstration in this work. The broadband designs of both the radiating unit and the feeding circuit are investigated in detail. The chokes are introduced in the metal grid plate to prevent leakage. After that, the SIW slot array and the metal grid plate with chokes are fabricated by the PCB and milling process, respectively. The prototype antenna is measured to verify the antenna operation and design.

II. ANTENNA CONFIGURATION

The configuration of the proposed 16×16-element broadband slot array antenna based on the single-layer SIW is illustrated in Fig. 1. It should be emphasized that both the feeding circuit and the radiating slots are appropriately integrated into one single substrate. The whole antenna is fed by a standard rectangular waveguide WR15 through a feed aperture. The grey area depicted in Fig. 1 represents the full-corporate feeding circuit by cascading serval H-plane T-junctions. We succeeded in making maximum use of the space by sharing the common post-walls between the adjacent SIWs. Each radiating slot is cut in the broad wall of each radiating waveguide, which is individually connected with one output of the feeding circuit. Owing to the corporate feed and structure symmetry, the path-lengths from the input aperture to all radiating slots are identical to each other without frequency dependence. In addition, every radiating slot can be independently excited by the feeding circuit with arbitrary amplitude and phase. It is evident that all radiating slots bear the same structural parameters, and it drastically simplified the antenna design. The metal grids function as open air-cavities for the radiating slots. The bandwidth for this cavity-loaded radiating slot can be significantly improved. The single-layer SIW slot array antenna with the metal grids can be fixed up only by screwing, since choke structures introduced on the backside of the metal grids can effectively prevent energy leakage.

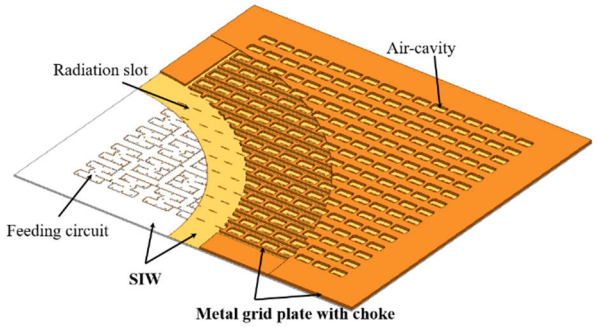

FIGURE 1. Configuration of the proposed 16 × 16-element array antenna.

III. ANTENNA DESIGN

The proposed single-layer full-corporate-fed structure features extending its feeding circuit output to every radiating slot. The slot spacing, as well as the waveguide width, has to be shortened to avoid the grating lobes. Hence, filling the waveguide with a dielectric material is one solution to ensure the dominant TE_{10} mode transmission. In this study, the Rogers substrate RT/duroid 6002 with a dielectric constant ε_r of 2.94 and a loss tangent tanδ of 0.0012 [23] is chosen as an example. The operating frequency range is supposed to be 57−66 GHz for FWA (Fixed Wireless Access) and WPAN (Wireless Personal Area Network) applications. At the center frequency of 61.5 GHz, the condition of dominant mode propagation is as follows [24]:

$$\frac{c}{2 \times f_{min} \times \sqrt{\varepsilon_r}} \leq a_d \leq \frac{c}{f_{max} \times \sqrt{\varepsilon_r}} \tag{1}$$

Here, a_d denotes the equivalent SIW width. c is the speed of light, while $f_{\min}$ and $f_{\max}$ are respectively 57 and 66 GHz in this work. According to [25], the slot spacing in both x- and y-directions should be no greater than 0.92 λ_0 to avoid the grating lobes. It is kept at 4.2 mm [9], which is about 0.92 λ_0 at the highest operating frequency of 66 GHz. The width a_d is optimized at 1.9 mm after full consideration, and it secures both the spatial arrangement and the power capacity.

The substrate thickness also plays an essential role in enhancing the antenna efficiency. The conductor loss can be significantly reduced by increasing the substrate thickness. It is an advantage over microstrip lines. As the typical value, 0.762 mm is chosen as the SIW thickness. It is a considerable value in the V-band, especially when compared with the typical thickness of microstrip lines. Meanwhile, the thickness of copper cladding after plating is fixed at 35 μm, identical to the thickness of radiating slots.

According to the corporate feed with high symmetry, the overall antenna can be roughly divided into two parts: the feeding circuit without slots and the 1 × 1-element subarray consisting of a single radiating slot. In theory, those two parts can be designed separately. The design procedures and simulated results are detailed as follows. The commercial electromagnetic-field simulation software Ansys HFSS is adopted in the antenna design.

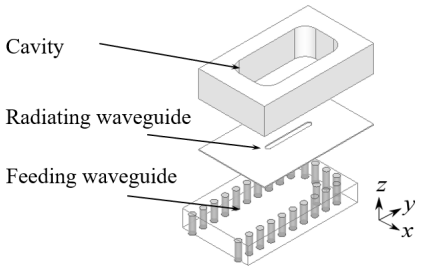

FIGURE 2. Exploded perspective view of the radiating slot.

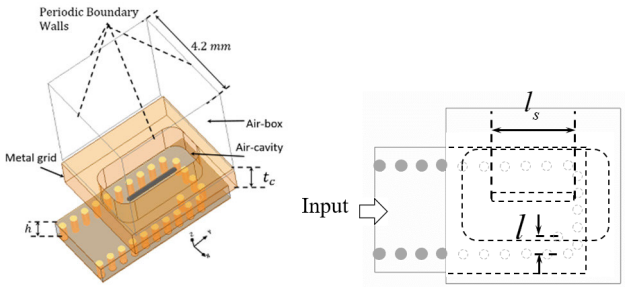

FIGURE 3. Analysis model of the radiating slot.

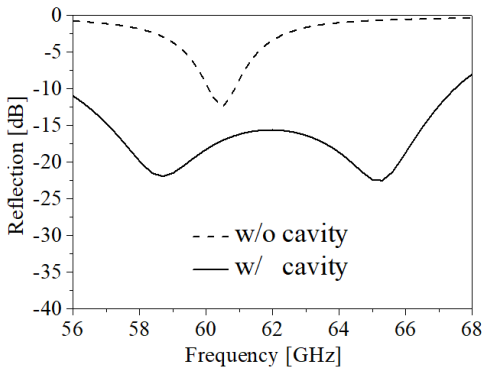

FIGURE 4. Reflection of the single radiating slot with and without air-cavity.

A. RADIATING SLOT

Fig. 2 shows the exploded perspective view of the single radiating slot as the primary design unit. Fig. 3 depicts its analysis model in Ansys HFSS. The radiating slot is placed one-quarter λ_g (guided wavelength) from the short end of the radiating waveguide and is offset from the waveguide axis to realize the desired excitation. Additionally, two pairs of periodic boundary walls are introduced in Fig. 3 (a) to simulate the mutual couplings in an infinite two-dimensional (2-D) slot array.

An extra post on the opposite side of the waveguide axis is introduced for input matching. However, its matching bandwidth is limited, as shown in Fig. 4, where a single resonance phenomenon is observed. The single slot without loading an air-cavity above suffers significantly from narrow matching bandwidth. To further improve the matching performance, an air-cavity is introduced above the slot additionally. These open air-cavities in a 2-D array can be easily realized by a

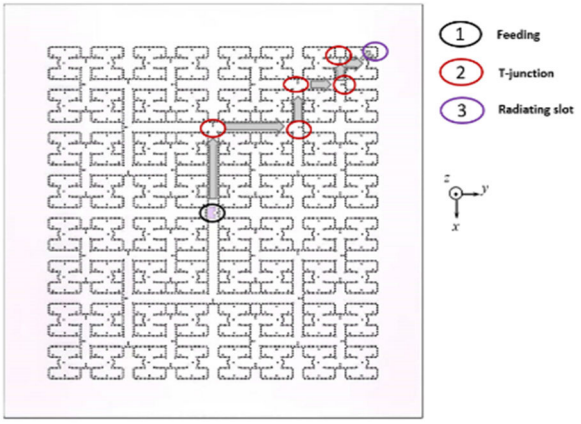

FIGURE 5. Plan view of the full-corporate feeding circuit.

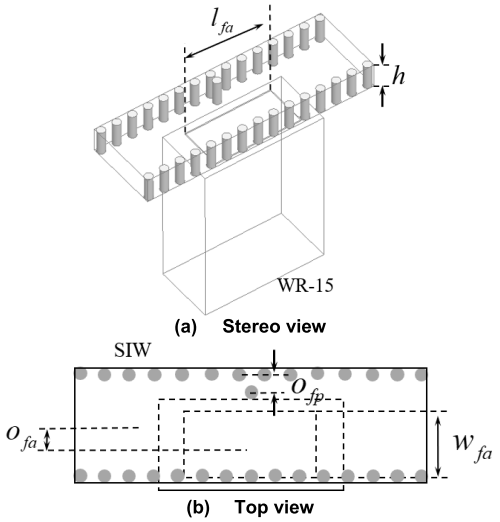

FIGURE 6. Analysis model of the WR-15 to SIW transition.

metal grid plate and be simply assembled with the SIW slot array only by screwing. Since the orientations of radiation slots and air-cavities are identical to each other, the metal grid does not affect the antenna polarization in this study. On the other hand, the metal grid can further serve as a polarization converter. By changing the shape and dimensions of the air-cavity, we can achieve desirable polarizations as well.

The simulated reflections of the single radiating slot with and without an air-cavity are summarized in Fig. 4 for comparison. It is observed that the bandwidth for $|S_{11}| < -15$ dB is improved from 3% to more than 16% by introducing an air-cavity. No critical sacrifice of the antenna profile is required since the total thickness remains as low as 0.41 λ_0 at 61.5 GHz.

B. FULL-CORPORATE FEEDING CIRCUIT

The plan view of the full-corporate feeding circuit is illustrated in Fig. 5. There are three key components. They are the WR-15 to SIW transition, the H-plane T-junction, and the H-junction, as respectively illustrated in Figs. 6, 7, and 8. The imaginary arrow in Fig. 5 shows one of the feeding paths from

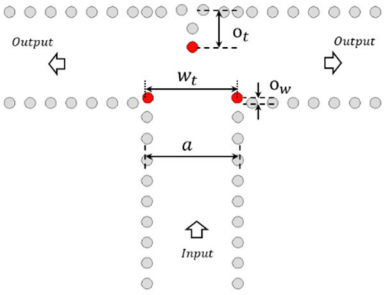

FIGURE 7. Analysis model of a T-junction.

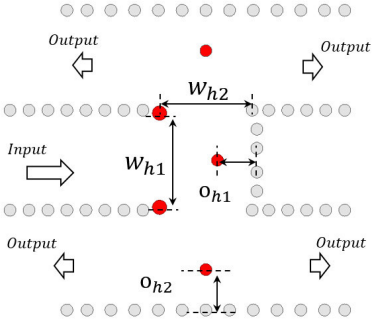

FIGURE 8. Analysis model of an H-junction.

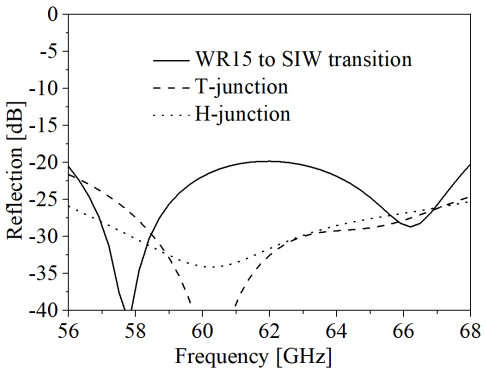

FIGURE 9. Reflection performance of three components.

the input aperture to one radiating slot. The corporate feeding circuit is formed by cascading a series of T-junctions. Good controllability in the feeding circuit's output power has been guaranteed for low sidelobe applications by optimizing the power division ratio in every T-junction.

Even though the WR-15 to SIW transition suffers from a large difference in the waveguide widths due to introducing high dielectric material in the substrate, a good matching bandwidth still can be achieved. After optimization in HFSS, the coupling aperture dimensions are determined at $l_{fa} = 2.73$ mm and $w_{fa} = 1.35$ mm, while the offsets of the input aperture and the matching post are determined at $o_{fa} = 0.39$ mm and $o_{fp} = 0.29$ mm. The simulated reflection shown in Fig. 9 is sufficiently suppressed below -20 dB over the frequency band ranging from 56 to 68 GHz. The matching performance of a single T-junction has a great effect on that of the overall feeding circuit. As shown in Fig. 7, several

extra matching posts are introduced to improve the matching bandwidth. Due to restrictions in both the SIW structure and the PCB process, the distance between the two posts should be larger than 0.2 mm + 0.25 mm = 0.45 mm. Here, 0.25 mm denotes the minimum diameter of a post. This restriction significantly degrades the matching bandwidth far from the best performance. The parameters shown in Fig. 7 are optimized at $o_t = 0.86$ mm, $w_t = 1.74$ mm, and $o_w = 0.12$ mm. Among those parameters, o_t and w_t are adjusted for good matching, whereas o_w is mainly adjusted for enough spacing between posts. The reflection of the designed T-junction is included in Fig. 9 as well. It is suppressed below −25 dB over frequency range of 57–67 GHz.

The feeding circuit and radiating slots are appropriately integrated within a single-layer substrate. We succeed in making maximum use of the space by sharing the common post-walls between the adjacent SIWs. As the tradeoff, we lose the design flexibility to some extent when cascading last two T-junctions into an H-junction. According to higher-order modes couplings, the overall H-junction has to be optimized slightly by HFSS. As illustrated in Fig. 8, several extra posts are introduced for good matching, and their positions and radius are optimized. The overall reflection is suppressed below −25 dB over the frequency range of 56−68 GHz, as included in Fig. 9 for comparison. The amplitude and phase variation among the four outputs of an H-junction are well suppressed below 0.6 dB and 0.5 degrees, respectively.

C. 2 × 2-ELEMENT SUBARRAY

After the designs of an H-junction and a radiating slot, we combine them into a 2 × 2-element subarray, as shown in Fig. 10. Due to the relatively compact structure, the structural parameters are necessary to be fine-tuned again. The values of those parameters before and after tuning are listed in Table 1. The overall reflection of a 2 × 2-element subarray after tuning is shown in Fig. 11, where the reflections of a radiating slot and an H-junction are reproduced and included for comparison. It is suppressed below −15 dB over the frequency band ranging from 57 to 66 GHz. The single radiating slot mainly restricts its bandwidth. It means the matching bandwidth of a 2 × 2-element subarray can be further enhanced by improving the radiating slot's matching performance. Nonetheless, the present bandwidth is sufficient to fully cover four channels for most wireless applications developed in the V-band [26].

It should be noted that the 2 × 2-element subarray designed above is totally different from that realized in [8]. As a future plan, it is scheduled to develop a 16 × 16-element low-sidelobe array by simply adjusting the power dividing ratios of T-junctions cascaded in the feeding circuit.

D. 16 × 16-ELEMENT ARRAY

The whole structure of a 16 × 16-element slot array formed by combining the radiating slot and the full-corporate feeding network is analyzed by HFSS. As shown in Fig. 12, the simulated overall reflection bandwidth for $|S_{11}| < -10$ dB is 16.2%. Besides, the reflections of a single T-junction and a 2 × 2-element subarray are included in Fig. 12 as well. It is obvious that the reflected waves from the radiating slots and cascaded T-junctions accumulate at the antenna input and determine the overall antenna reflection.

With the consideration of antenna assembly by screwing, a small air gap may exist between the substrate and the metal grid plate. It leads to imperfect electric contact as well as to power leakage. To prevent the E-orientation power leakage,

TABLE 1. Antenna structural parameters before and after tuning.

Structual parameters	Before	After
Width of the cavity in x-direction	1.79	2.19
Length of the cavity in y-direction	3.52	3.52
Height of the cavity: t_c	1.2	1.24
Width of the slot: w_s	0.21	0.14
Length of the slot: l_s	2.07	1.9
Offset distance of the slot	0.43	0.33
Offset distance of the post in x-direction	0.42	0.45
Offset distance of the post in y-direction	0.82	0.62
Width w_{h1} in the 1st T-junc. in Fig. 8	1.98	1.94
Offset distance o_{h1} in the 1st T-junc. in Fig. 8	0.83	0.8
Width w_{h2} in the 2nd T-junc. in Fig. 8	1.95	1.95
Offset distance o_{h2} in the 2nd T-junc. in Fig. 8	0.85	0.57

(UNIT: MM)

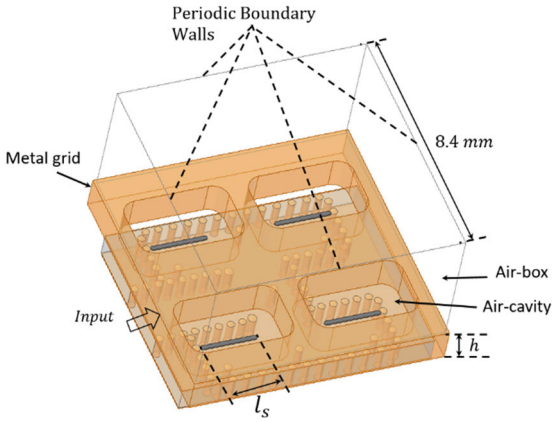

FIGURE 10. Simulation model of 2 × 2-element subarray.

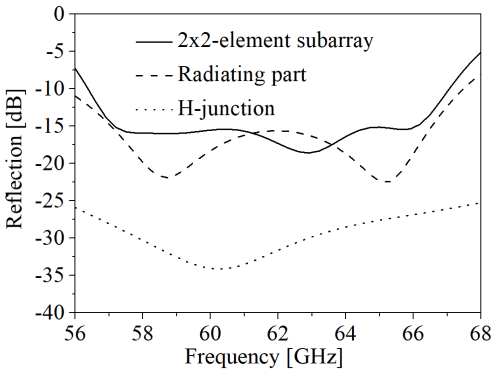

FIGURE 11. Reflection performance of a 2 × 2-element subarray.

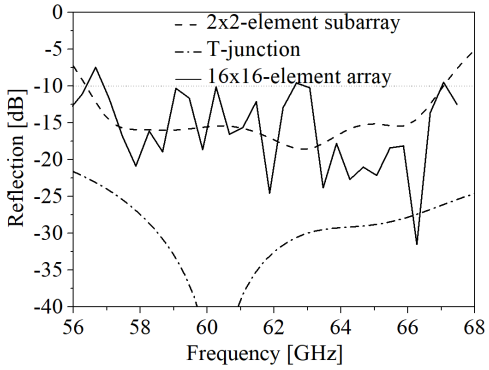

FIGURE 12. Simulated overall reflection of a 16 × 16-element array.

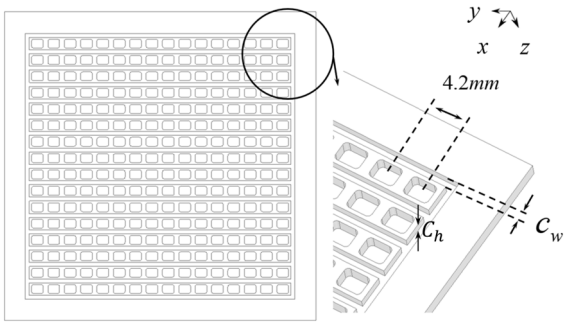

FIGURE 13. Designed choke below the metal grid layer.

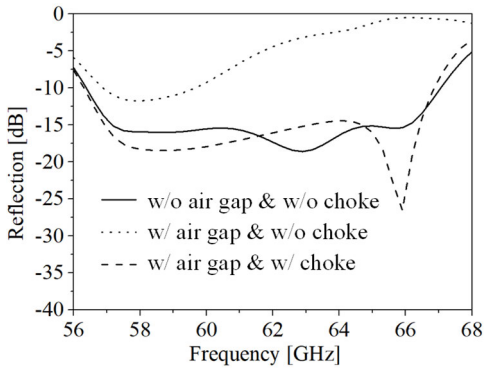

FIGURE 14. Designed choke below the metal grid layer.

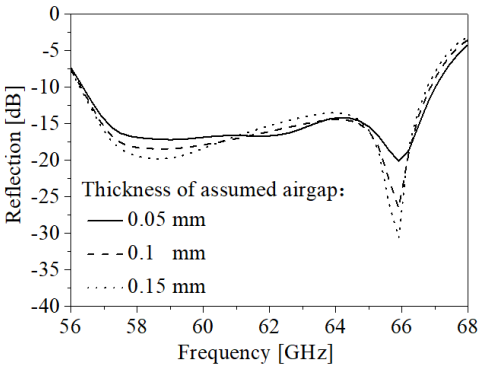

FIGURE 15. Designed choke below the metal grid layer.

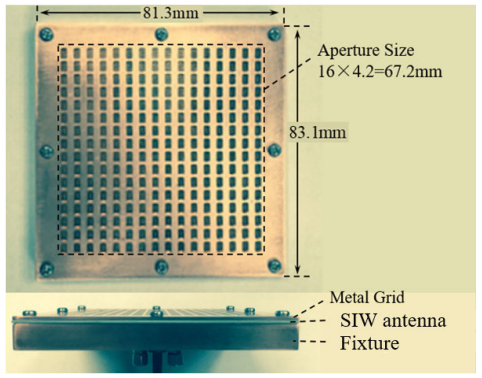

FIGURE 16. Picture of the fabricated antenna.

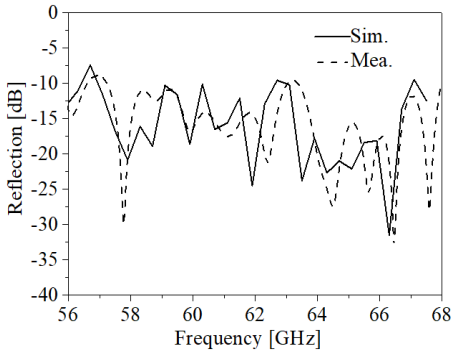

FIGURE 17. Simulated and measured reflections of the 16 × 16-element slot array.

we introduce a series of H-orientation chokes on the backside of the metal grid plate. As illustrated in Fig. 13, those chokes lie in the middle of the adjacent cavities. Another choke surrounding the antenna aperture is introduced as well. However, there is not enough space to introduce two-dimensional chokes. Assuming the air gap thickness of 0.1 mm, we design the choke based on a 2 × 2-element subarray model. The depth C_h and width C_w of the choke are optimized at 1 mm in common. The reflections of 2 × 2-element subarrays with and without choke are summarized in Fig. 14 for comparison. The introduction of chokes compensates for the imperfect electric contact to a certain extent. The dependence on air gap thickness is investigated as well. The reflections of 2 × 2-element subarrays with different air gap thicknesses are simulated and summarized in Fig. 15 for comparison. It is well verified that the operation of chokes is stable with negligible dependence on the air gap thickness.

IV. ANTENNA FABRICATION AND EVALUATION

The proposed 16 × 16-element single-layer SIW slot array designed in the 60-GHz band is fabricated by the traditional PCB process, whereas the metal grid plate is fabricated the milling process [27]. Unfortunately, we failed in the first trial fabrication. The minimum diameter and the minimum spacing between a slot and a through via are restricted to 0.2 mm. The evaluation results of the refabricated test antenna are reported in this paper. The overall antenna size is 81.3 mm × 83.1 mm, and 16.6 λ_0× 17 λ_0 at 61.5 GHz. The antenna aperture area is defined as 67.2 mm

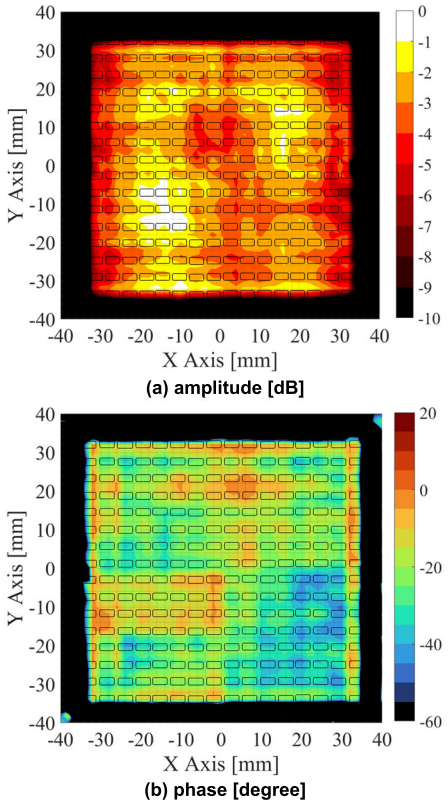

FIGURE 18. Measured aperture distributions at 61.5 GHz.

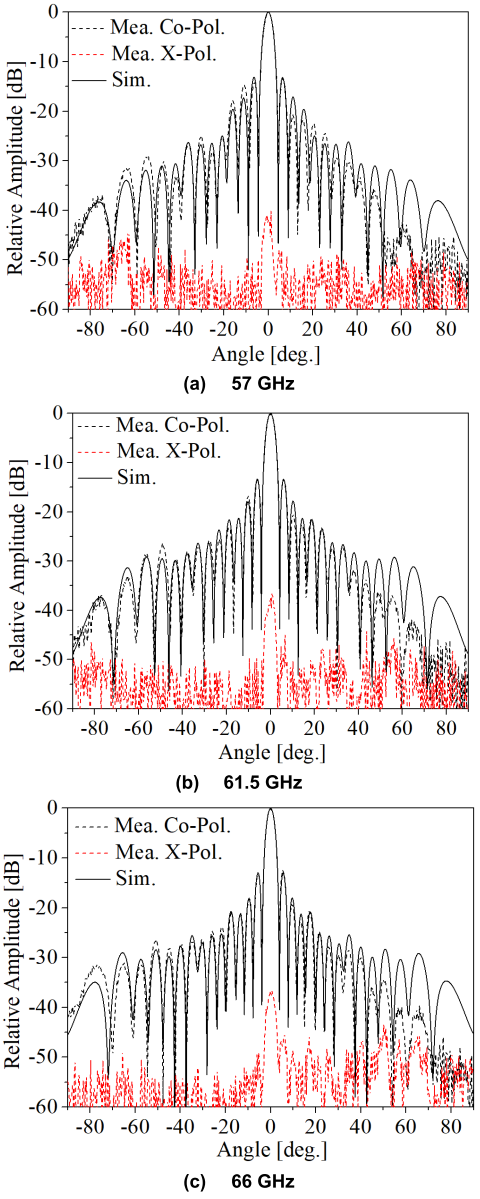

FIGURE 19. *H*-plane radiation patterns at different frequencies.

(= 4.2 mm ×16) square. Fig. 16 shows the photograph of a test antenna installed on an assembly jig is connected to the flange of WR-15. The SIW slot array is sandwiched between the metal grid with 1.24-mm thickness and the assembly jig with 8-mm thickness. They are assembled only by screwing at the periphery. We evaluate the antenna performances in detail.

A. REFLECTION

Before the measurement, the standard waveguide WR-15 is calibrated at its interface using the most popular TOSM (Through Open Short Match) method. The frequency characteristic of the overall reflection measured by a vector network analyzer is shown in Fig. 17. The reflection of the test antenna is suppressed below −10 dB over the frequency range of 57−67.5 GHz. The simulated reflection is also included in Fig. 17 for comparison. A good agreement between the simulated and measured results is observed. A small discrepancy may come from manufacturing and assembling tolerance.

B. APERTURE FIELD DISTRIBUTIONS

We measure the aperture distributions of the test antenna under a planar near-field measurement system. Fig. 18 shows the amplitude and phase of the aperture distributions at the center frequency of 61.5 GHz. The deviations in amplitude and phase are suppressed within 5 dB and 40 degrees, respectively. According to our investigation, there are two contributions to non-uniformity in the excitation: one is due to the slots lying at the antenna periphery; the other is due to the uneven thickness of the air gap between the substrate and the metal grid plate. Nonetheless, the limited non-uniformity in aperture distribution cannot cause significant degradation in directivity.

C. RADIATION PATTERNS

The far-field antenna radiation patterns are measured in an anechoic chamber. The *H*-plane radiation patterns at 57, 61.5, and 66 GHz are summarized in Fig. 19, where the simulated results are also included for comparison. It is obvious that the simulated and measured results have a good agreement with each other for all frequencies. The measured and simulated *E*-plane radiation patterns are summarized in Fig. 20

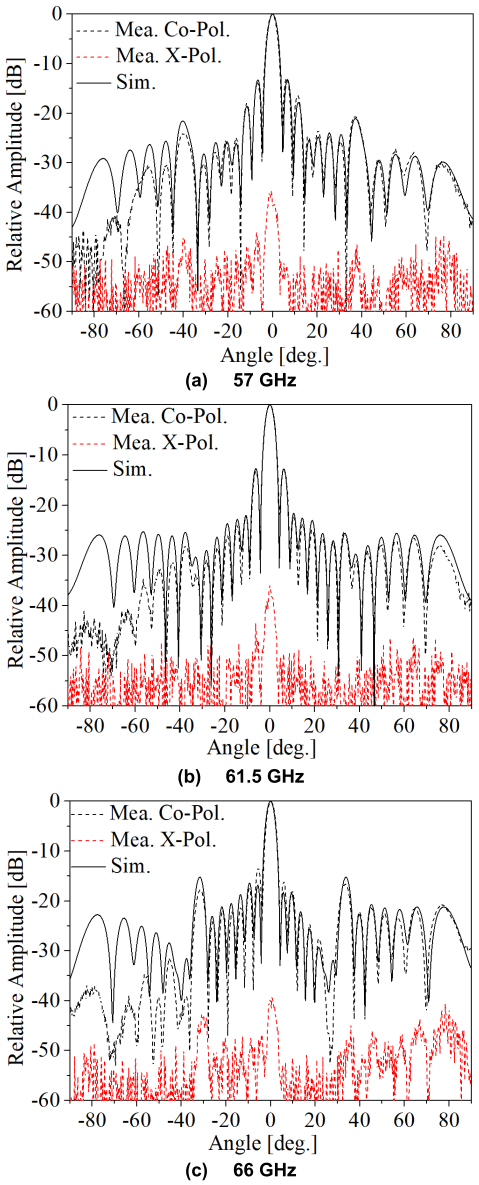

FIGURE 20. *E*-plane radiation patterns at different frequencies.

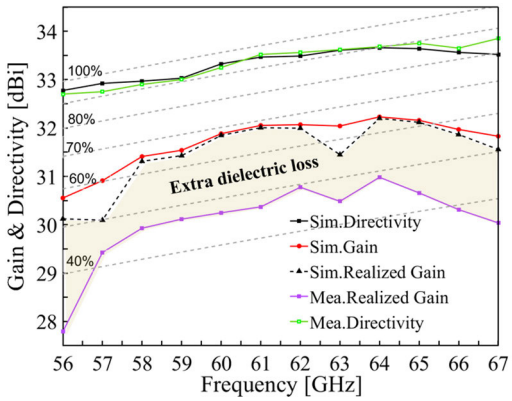

FIGURE 21. Simulated and measured directivities and antenna gains.

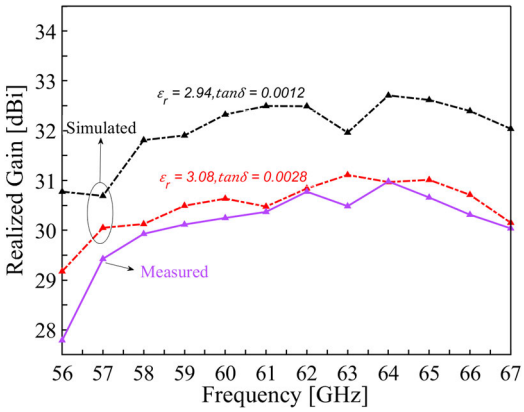

FIGURE 22. Comparison of simulated and measured on antenna gains.

for comparison. Relatively high sidelobes are observed at ±30–40 degrees when the operation frequency deviates from 61.5 GHz. The slots, as well as the air-cavities strongly couple with each other, especially along the *E*-plane direction. Since the aperture size of the air-cavity is large, the field distribution on its aperture is not uniform. This phenomenon contributes to the degradation of sidelobes. In both *E*- and *H*-planes, the measured cross-polarizations are well suppressed below −40 dB for all frequencies.

D. GAIN AND EFFICIENCY

The frequency characteristics of the measured and simulated directivities, gains, and realized gains are summarized in Fig. 21, where corresponding efficiencies are also included. The measured directivity is calculated by Fourier transforming from the measured near-field distributions. The realized gain of the test antenna is measured in an anechoic chamber by comparing with a standard-gain horn antenna. The measured and simulated directivities coincide well with each other. The simulated realized gain is higher than 31.5 dBi, and its corresponding aperture efficiency is higher than 65% over the frequency range of 59–66 GHz. Meanwhile, the measured realized gain is higher than 30 dBi, and its corresponding antenna efficiency is higher than 45% over the frequency range of 58–66 GHz. According to our investigation, the main contribution to the critical degradation in the measured realized gain comes from the actual loss tangent of RT/duroid 6002 in the V-band, which must be much larger [27] than that listed in the catalog. According to [28], its dielectric constant and loss tangent are respectively 3.08 and 0.0028 in the V-band. We re-simulated the 16×16-element single-layer SIW slot array antenna with the updated dielectric properties. For comparison, the realized gains for different material parameters are summarized in Fig. 22, where good agreement between the measured and re-simulated realized gains is observed. Hence, the reliability of the data reported in [28] is also confirmed by our test antenna.

A few types of corporate-fed slot array antennas have been successfully developed in the 60-GHz band. Their configurations and antenna performances are investigated and summarized in Table 2 for comparison. Our proposed antenna has achieved low-profile, low-cost, broadband, high-gain,

TABLE 2. Comparison between the proposed and reported 60-GHz planar antenna arrays.

Ref.	Number of Elements in an array	Antenna Layers	Number of elements in a subarray	Frequency Band (GHz)	Bandwidth (VSWR < 2)	Gain (dBi)	Antenna Efficiency	Fabrication Technique (Antenna Structure)
[9]	16×16	Double	2×2	59.0-64.0	13.0%	33	80%-85%	Diffusion bonding (hollow waveguide)
[11]	16×16	Double	2×2	56.0-65.7	16.0%	32.5	70%-90%	Milling (gap waveguide)
[14]	16×16	Double	2×2	57.5-67.0	15.3%	30.1	<49.5%	PCB (cavity backed patch)
[16]	8×8	Multiple	1×2	54.8-65.1	17.1%	22.1	44.4%	LTCC (SIW)
[18]	16×16	Single	1×1	58.0-64.5	10.0%	32.5	70%-75%	Diffusion bonding (hollow rectangular coaxial line)
[19]	8×8	Single	1×1	56.5-67.0	17.0%	27	70%-85%	Milling (gap waveguide)
[21]	4×4	Multiple	1×1	53.0-67.0	22.6%	19.6	<54.5%	PCB (cavity backed patch)
This work	16×16	Single	1×1	57.0-67.0	16.2%	31	40%-50%	PCB (SIW)

high-efficiency characteristics. Besides, a broadband radial-line slot array antenna has been successfully developed by introducing a radially nonuniform TEM waveguide [29]. By compromising on the aperture efficiency at about 30%, the test antenna exhibits an extremely broad bandwidth of 27.6% for both AR (Axial Ratio) < 3 dB and $|S_{11}| < -10$ dB.

V. CONCLUSION

A full-corporate-fed single-layer SIW slot array is newly proposed and verified. A 16×16-element array is designed in the V-band for demonstration. The test antenna is composed of a slotted SIW and a metal grid plate. They are fabricated respectively by PCB and milling processes. As the evaluation results, the measured bandwidth for $|S_{11}| < -10$ dB is 16.2%, fully covering the 57–67 GHz frequency range. Meanwhile, the measured realized gain higher than 30 dBi associated with the antenna efficiency higher than 45% is achieved over the 58−65 GHz frequency range. It is verified that a low-profile, low-cost, broadband, high-gain, high-efficiency slot array antenna has been successfully developed in the V-band.

REFERENCES

[1] Y. P. Zhang and D. Liu, "Antenna-on-chip and antenna-in-package solutions to highly integrated millimeter-wave devices for wireless communications," *IEEE Trans. Antennas Propag.*, vol. 57, no. 10, pp. 2830–2841, Oct. 2009.

[2] Y. Kim, Y. Miura, T. Shirosaki, T. Taniguchi, Y. Kazama, J. Hirokawa, M. Ando, and T. Shirouzu, "A low-cost and very compact wireless terminal integrated on the back of a waveguide planar array for 26 GHz band fixed wireless access (FWA) systems," *IEEE Trans. Antennas Propag.*, vol. 53, no. 8, pp. 2456–2463, Aug. 2005.

[3] R. Kreutel, "The hyperboloidal lens with laterally displaced dipole feed," *IEEE Trans. Antennas Propag.*, vol. AP-28, no. 4, pp. 443–450, Jul. 1980.

[4] P. Hannan, "Microwave antennas derived from the Cassegrain telescope," *IRE Trans. Antennas Propag.*, vol. 9, no. 2, pp. 140–153, Mar. 1961.

[5] E. Levine, G. Malamud, S. Shtrikman, and D. Treves, "A study of microstrip array antennas with the feed network," *IEEE Trans. Antennas Propag.*, vol. 37, no. 4, pp. 426–434, Apr. 1989.

[6] M. Ando, Y. Tsunemitsu, M. Zhang, J. Hirokawa, and S. Fujii, "Reduction of long line effects in single-layer slotted waveguide arrays with an embedded partially corporate feed," *IEEE Trans. Antennas Propag.*, vol. 58, no. 7, pp. 2275–2280, Jul. 2010.

[7] S. Park, Y. Tsunemitsu, J. Hirokawa, and M. Ando, "Center feed single layer slotted waveguide array," *IEEE Trans. Antennas Propag.*, vol. 54, no. 5, pp. 1474–1480, May 2006.

[8] S. Fujii, Y. Tsunemitsu, G. Yoshida, N. Goto, M. Zhang, J. Hirokawa, and M. Ando, "A wideband single-layer slotted waveguide array with an embedded partially corporate feed," in *Proc. Int. Symp. Antennas Propag.*, Oct. 2008, pp. 1–4.

[9] Y. Miura, J. Hirokawa, M. Ando, Y. Shibuya, and G. Yoshida, "Double-layer full-corporate-feed hollow-waveguide slot array antenna in the 60-GHz band," *IEEE Trans. Antennas Propag.*, vol. 59, no. 8, pp. 2844–2854, Aug. 2011.

[10] J. Hirokawa, M. Zhang, Y. Miura, and M. Ando, "High-efficiency wide-band double-layer slotted hollow waveguide array antennas by diffusion bonding of laminated thin metal plates," in *Proc. 20th Int. Conf. Appl. Electromagn. Commun. (ICECom)*, Dubrovnik, Croatia, 2010, pp. 1–4.

[11] D. Zarifi, A. Farahbakhsh, A. U. Zaman, and P. S. Kildal, "Design and fabrication of a high-gain 60-GHz corrugated slot antenna array with ridge gap waveguide distribution layer," *IEEE Trans. Antennas Propag.*, vol. 64, no. 7, pp. 2905–2913, Jul. 2016.

[12] S. M. Sifat, M. M. M. Ali, S. I. Shams, and A.-R. Sebak, "High gain bow-tie slot antenna array loaded with grooves based on printed ridge gap waveguide technology," *IEEE Access*, vol. 7, pp. 36177–36185, 2019.

[13] D. F. Guan, Z. P. Qian, Y. S. Zhang, and J. Jin, "High-gain SIW cavity-backed array antenna with wideband and low sidelobe characteristics," *IEEE Antennas Wireless Propag. Lett.*, vol. 14, pp. 1774–1777, 2015.

[14] J. Wu, Y. J. Cheng, and Y. Fan, "60-GHz substrate integrated waveguide fed cavity-backed aperture-coupled microstrip patch antenna arrays," *IEEE Trans. Antennas Propag.*, vol. 63, no. 3, pp. 1075–1085, Mar. 2015.

[15] J. Wu, Y. J. Cheng, and Y. Fan, "A wideband high-gain high-efficiency hybrid integrated plate array antenna for V-band inter-satellite links," *IEEE Trans. Antennas Propag.*, vol. 63, no. 4, pp. 1225–1233, Apr. 2015.

[16] J. F. Xu, Z. N. Chen, X. M. Qing, and W. Hong, "Bandwidth enhancement for a 60 GHz substrate integrated waveguide fed cavity array antenna on LTCC," *IEEE Trans. Antennas Progag.*, vol. 59, no. 3, pp. 826–832, Mar. 2011.

[17] Y. Watarai, M. Zhang, J. Hirokawa, and M. Ando, "Sidelobe suppression in a corporate-feed double-layer waveguide slot array antenna," in *Proc. Int. Symp. Antennas Propag.*, Jeju, South Korea, Oct. 2011, pp. 1–4.

[18] M. Sano, J. Hirokawa, and M. Ando, "Single-layer corporate-feed slot array in the 60-GHz band using hollow rectangular coaxial lines," *IEEE Trans. Antennas Propag.*, vol. 62, no. 10, pp. 5068–5075, Oct. 2014.

[19] J. Liu, A. Vosoogh, A. U. Zaman, and J. Yang, "A slot array antenna with single-layered corporate-feed based on ridge gap waveguide in the 60 GHz band," *IEEE Trans. Antennas Propag.*, vol. 67, no. 3, pp. 1650–1658, Mar. 2019.

[20] W. Y. Yong, T. Emanuelsson, and A. A. Glazunov, "5G wideband magneto-electric dipole antenna fed by a single-layer corporate-feed network based on ridge gap waveguide," in *Proc. 14th Eur. Conf. Antennas Propag. (EuCAP)*, Mar. 2020, pp. 1–4.

[21] Y. Li and K.-M. Luk, "Low-cost high-gain and broadband substrate-integrated-waveguide-fed patch antenna array for 60-GHz band," *IEEE Trans. Antennas Propag.*, vol. 62, no. 11, pp. 5531–5538, Nov. 2014.
[22] B. Duan, M. Zhang, J. Hirokawa, and Q. Huo Liu, "Subarray design of a single-layer corporate-fed dielectric-filled waveguide slot array antenna," in *Proc. 12th Eur. Conf. Antennas Propag. (EuCAP)*, London, U.K., 2018, pp. 1–2.
[23] Rogers Corporation, Chandler, AZ, USA. *RT/Duroid 6002 Laminates*. [Online]. Available: https://www.rogerscorp.com/advanced-electronics-solutions/rt-duroid-laminates/rt-duroid-6002-laminates
[24] A. S. Khan, *Microwave Engineering: Concepts and Fundamentals*. Boca Raton, FL, USA: CRC Press, 2014, ch. 3.
[25] R. C. Johnson and H. Jasik, *Antenna Engineering Handbook*. New York, NY, USA: McGraw-Hill, 1984, ch. 9.
[26] H. B. H. Dutty and M. M. Mowla, "Channel modeling at unlicensed millimeter wave v band for 5G backhaul networks," in *Proc. 5th Int. Conf. Adv. Electr. Eng. (ICAEE)*, Dhaka, Bangladesh, Sep. 2019, pp. 769–773.
[27] M. Zhang, B. Duan, J. Hirokawa, Q. H. Liu, and G.-L. Huang, "A 16 × 16-element single-layer full-corporate-fed SIW slot array antenna," in *Proc. 14th Eur. Conf. Antennas Propag. (EuCAP)*, Mar. 2020, pp. 1–3.
[28] C. D. Morcillo, S. K. Bhattacharya, A. Horn, and J. Papapolymerou, "Thermal stability of the dielectric properties of the low-loss, organic material RT/duroid 6002 from 30 GHz to 70 GHz," in *Proc. 60th Electron. Compon. Technol. Conf. (ECTC)*, Las Vegas, NV, USA, 2010, pp. 1830–1833.
[29] M. N. Y. Koli, M. U. Afzal, and K. P. Esselle, "Significant bandwidth enhancement of radial-line slot array antennas using a radially nonuniform TEM waveguide," *IEEE Trans. Antennas Propag.*, vol. 69, no. 6, pp. 3193–3203, Jun. 2021.

BAOQUAN DUAN (Graduate Student Member, IEEE) was born in Anhui, China, in 1993. He received the B.S. degree in electronic information engineering from the Hefei University of Technology (HFUT), Anhui, in 2016, and the M.S. degree in electronics and communication engineering from Xiamen University (XMU), Fujian, China, in 2019. He is currently pursuing the D.E. degree with the Tokyo Institute of Technology, Tokyo, Japan.

His research interest includes high-gain millimeter-wave antennas.

SHIJIU ZHENG was born in Yunnan, China, in 1998. He received the B.S. degree in electromagnetic and wireless technology from Xiamen University (XMU), Fujian, China, in 2022, where he is currently pursuing the M.S. degree. His research interests include waveguide slot antennas and antennas for the Internet of Things (IoT) applications.

MIAO ZHANG (Senior Member, IEEE) received the B.S., M.S., and D.E. degrees in electrical and electronic engineering from the Tokyo Institute of Technology, Tokyo, Japan, in 2003, 2005, and 2008, respectively.

From 2005 to 2008, he was a Research Fellow with the Japan Society for the Promotion of Science, Tokyo. Since 2008, he has been a Postdoctoral Researcher with the Tokyo Institute of Technology, and he became an Assistant Professor, in 2013. From 2016 to 2022, he was an Associate Professor at Xiamen University, Fujian, China, where he is currently a Professor. His research interests include waveguide slot arrays, millimeter-wave antennas, and array antennas for 5G and car-radar applications.

Dr. Zhang is a Senior Member of CIE and IEICE. He was a recipient of the Best Letter Award from IEICE Communication Society, in 2009; the Young Engineer Award from IEICE Technical Committee on Antennas and Propagation, in 2010; the IEEE AP-S Japan Chapter Young Engineer Award, in 2011; and the Best Paper Award at the 9th European Conference on Antennas and Propagations, in 2015.

JIRO HIROKAWA (Fellow, IEEE) was born in Tokyo, Japan, in 1965. He received the B.S., M.S., and D.E. degrees in electrical and electronic engineering from the Tokyo Institute of Technology (Tokyo Tech), Tokyo, in 1988, 1990, and 1994, respectively.

He was a Research Associate and an Associate Professor at Tokyo Tech, from 1990 to 1996 and from 1996 to 2015, respectively, where he is currently a Professor. He was with the Antenna Group, Chalmers University of Technology, Gothenburg, Sweden, as a Postdoctoral Fellow, from 1994 to 1995. He has authored or coauthored more than 200 peer-reviewed journal articles and more than 600 international conference presentations. His current research interests include analyses, designs, and fabrication techniques of slotted waveguide array antennas, millimeter-wave, terahertz antennas, and beam-switching circuits. He is a fellow of IEICE. He received IEEE AP-S Tokyo Chapter Young Engineer Award, in 1991; the Young Engineer Award from IEICE, in 1996; the Tokyo Tech Award for Challenging Research, in 2003; the Young Scientists' Prize from the Minister of Education, Cultures, Sports, Science and Technology, Japan, in 2005; the Best Paper Award, in 2007; the Best Letter Award from IEICE Communications Society, in 2009; and IEICE Best Paper Award, in 2016 and 2018. He was the Chair of the Technical Program Committee for ISAP 2016. He was also the Chair of IEICE Technical Committee on Antennas and Propagation, from 2017 to 2019. He served as an Associate Editor for *IEICE Transactions on Communications* from 1999 to 2003 and from 2004 to 2007. He also served as an Associate Editor (2013–2016) and a Track Editor (2016–2022) for IEEE TRANSACTIONS ON ANTENNAS AND PROPAGATION.

QING HUO LIU (Fellow, IEEE) received the B.S. and M.S. degrees in physics from Xiamen University, Xiamen, China, in 1983 and 1986, respectively, and the Ph.D. degree in electrical engineering from the University of Illinois at Urbana–Champaign, Champaign, IL, USA, in 1989.

He was with the Electromagnetics Laboratory, University of Illinois Urbana–Champaign, as a Research Assistant, from September 1986 to December 1988, and a Postdoctoral Research Associate, from January 1989 to February 1990. He was a Research Scientist and a Program Leader with Schlumberger-Doll Research, Ridgefield, CT, USA, from 1990 to 1995. From 1996 to May 1999, he was an Associate Professor with New Mexico State University, Las Cruces, NM, USA. From 1999 to 2022, he was a tenured Full Professor of electrical and computer engineering with Duke University, Durham, NC, USA. He is currently a Chair Professor with the Eastern Institute for Advanced Study and a Visiting Chair Professor with Xiamen University. His research interests include computational electromagnetics and acoustics, inverse problems, and their applications in nanophotonics, geophysics, biomedical imaging, and electronic design automation. He has authored widely in these areas.

Dr. Liu is a fellow of the Acoustical Society of America, the Electromagnetics Academy, and the Optical Society of America. He received the 1996 Presidential Early Career Award for Scientists and Engineers (PECASE) from the White House, the 1996 Early Career Research Award from the Environmental Protection Agency, and the 1997 CAREER Award from the National Science Foundation. He received the 2017 Technical Achievement Award and the 2018 Computational Electromagnetics Award from the Applied Computational Electromagnetics Society and the 2018 Harrington-Mittra Award in Computational Electromagnetics from the IEEE Antennas and Propagation Society. In 2018, he received the University of Illinois Urbana–Champaign ECE Distinguished Alumni Award. He served as an IEEE Antennas and Propagation Society Distinguished Lecturer and the Founding Editor-in-Chief for the IEEE JOURNAL ON MULTISCALE AND MULTIPHYSICS COMPUTATIONAL TECHNIQUES, from 2015 to 2018.